



1 **Atmospheric Water-Soluble Organic Nitrogen (WSON) in the Eastern Mediterranean:**

2 **Origin and Ramifications Regarding Marine Productivity**

3 **Münevver Nehir¹ and Mustafa Koçak^{1*}**

4

5 ¹ Institute of Marine Sciences, Middle East Technical University, P.O. Box 28, 33731,

6 Erdemli-Mersin, Turkey

7 *Corresponding author (Tel: +90324-5213434; Fax: +90324-5212327;

8 mkocak@ims.metu.edu.tr

9

10 **Abstract**

11 Two-sized aerosol and rain sampling were carried out at a rural site located on the coast of the
12 Eastern Mediterranean, Erdemli, Turkey (36° 33' 54" N and 34° 15' 18" E). A total of 674
13 aerosol samples in two size fraction (coarse = 337; fine = 337) and 23 rain samples were
14 collected between March 2014 and April 2015. Samples were analyzed for NO₃⁻, NH₄⁺ and
15 ancillary water-soluble ions by Ion Chromatography and water-soluble total nitrogen (WSTN)
16 by applying a High Temperature Combustion Method. The mean aerosol WSON was 23.8 ±
17 16.3 nmol N m⁻³, reaching a maximum of 79 nmol N m⁻³, with about 66 % being associated
18 with coarse particles. The volume weighted mean (VWM) concentration of WSON in rain
19 was 21.5 μmol N L⁻¹. The WSON contributed 37 % and 29 % to the WSTN in aerosol and
20 rainwater, respectively. Aerosol WSON concentrations exhibited large temporal variations
21 mainly due to rain and the origin of air mass flow. The highest mean aerosol WSON
22 concentration was observed in the summer and was attributed to the absence of rain and re-
23 suspension of cultivated soil in the region. The mean concentration of WSON during dust
24 events (38.2±17.5 nmol N m⁻³) was 1.3 times higher than that of non-dust events (29.4±13.9
25 nmol N m⁻³). Source apportionment analysis demonstrated that WSON was originated from
26 agricultural activities (43 %), secondary aerosol (20 %), nitrate (22 %), crustal (10 %) and
27 sea-salt (5 %). The dry and wet depositions of WSON were equivalent and amounted to 36 %
28 of the total atmospheric WSTN flux. Considering the Cilician Basin, the atmospheric water-
29 soluble nitrogen flux would sustain 33 % and 76 % of the new production in the associated
30 coastal and open waters, respectively.

31

32 **Keywords:** Atmospheric water-soluble organic nitrogen, mineral dust, source apportionment,
33 atmospheric deposition and marine productivity, Eastern Mediterranean

34



35 1. Introduction

36 Research assessing the atmospheric deposition of nitrogen (with a focus on inorganic
37 N in rainwater i.e. ammonium and nitrate) can be traced back to the mid-1800s (Miller, 1995
38 and references therein) as it was accepted to be a vital plant nutrient. Miller (1905) mentioned
39 about organic nitrogen in rain samples as well. To quote Miller: ‘*With regard to the amount of*
40 *organic nitrogen in the rainwater, the only available analyses relating to Rothamsted are*
41 *those of Frankland who found from 0.03 to 0.66 per million in 69 samples*’. Cornell et al.,
42 (1995) highlighted the importance of organic nitrogen in rain and snow accounting for almost
43 half of the total atmospheric dissolved nitrogen deposition. Since then, research defining the
44 quantitative importance of soluble organic nitrogen in the atmospheric transport of nitrogen
45 has greatly expanded (Neff et al, 2002; Cornell et al., 2003; Mace et al., 2003a, b, c; Gilbert et
46 al., 2005; Sorooshian et al., 2008; Violaki and Mihalopoulos, 2010; Violaki et al., 2010;
47 Altieri et al., 2016).

48 WSON arises from a variety of sources including both natural and anthropogenic.
49 Anthropogenic sources include agricultural activities (including fertilizer application, animal
50 husbandry), high temperature fossil fuel combustion, man-made biomass burning and
51 industrial activities. In contrast natural sources of WSON include mineral dust, bacteria, sea
52 salt, organic debris, natural biomass burning (Neff et al, 2002; Cornell et al., 2003; Mace et
53 al., 2003a, b, c; Gilbert et al., 2005; Sorooshian et al., 2008; Altieri et al., 2016). Atmospheric
54 organic nitrogen can also be formed through chemical reactions. For example, reactions
55 between volatile organic compounds, NO_x and ammonium sulfate aerosols may lead to the
56 formation of nitrogen-containing compounds (Surratt et al., 2008; Galloway et al., 2009; De
57 Haan et al., 2011; Yu et al., 2011). Furthermore, atmospheric organic nitrogen plays an
58 essential role in many global processes which may impact on the chemistry of the atmosphere
59 as well as climate and biogeochemical cycles. Similar to ammonium, organic nitrogen species



60 such as urea and amines have acid-neutralizing capacities (Ge et al., 2011). It has been shown
61 that nitrogen containing organic compounds nucleate cloud droplets and may contribute
62 considerably to the indirect aerosol effect (Twohy et al., 2005). Phytoplankton and bacteria
63 production in aquatic environments has been found to be stimulated by the addition of water-
64 soluble organic nitrogen (Timperly et al., 1985; Peierlt and Paerl, 1997; Seitzinger and
65 Sanders, 1999). The laboratory experiments performed by Seitzinger and Sanders (1999)
66 demonstrated production of coastal marine bacteria and phytoplankton which are stimulated
67 by the addition of water-soluble organic nitrogen, 45-75 % being Bioavailable. From the mid
68 1800s to 2000, as a result of anthropogenic activities, reactive nitrogen and reactive
69 anthropogenic organic nitrogen have increased by almost 10 and 4 fold, respectively, leading
70 to a significantly modified global nitrogen cycle. This in term has impacted upon the marine
71 nitrogen biogeochemical cycling (Galloway et al., 2002, 2008; Duce et al., 2008).

72 The Mediterranean Sea is characterized by oligotrophic surface waters with Low
73 Nutrient Low Chlorophyll (LNLC) regions. This has been attributed to mainly anti-estuarine
74 (reverse thermohaline) circulation (Hamad et al., 2005). The Eastern Mediterranean (25) has
75 higher molar N/P ratios than those observed in the Western Mediterranean (22) and the
76 Redfield ratio (Krom et al., 2004; Yılmaz and Tuğrul, et al., 1998). It has been proposed that
77 the primary productivity in the Eastern Mediterranean is phosphorous limited (Thingstad et al.,
78 2005). However it has also been suggested that the primary productivity and bacterial activity
79 in the Eastern Mediterranean is limited by nitrogen or co-limited by nitrogen and phosphorous
80 (Yücel, 2013; Yücel, 2017). Very little research has focused on the importance of water-
81 soluble organic nitrogen inputs to marine productivity in the Eastern Mediterranean (Violaki
82 and Mihalopoulos, 2010; Violaki et al., 2010). Hence, the unique contributions of the current
83 study will be to (i) define the temporal variability of atmospheric water-soluble organic
84 nitrogen, (ii) assign the origin of the water-soluble organic nitrogen, (iii) assess the influence



85 of mineral dust on water-soluble organic nitrogen and (iv) enhance our knowledge of the
86 quantitative dry and wet deposition for water-soluble organic nitrogen and its possible
87 influence on marine productivity in the North Eastern Mediterranean.

88 These will be achieved by using the acquired data from the analyses for water soluble
89 inorganic and organic nitrogen species of a series of size fractionated aerosol (coarse and fine)
90 and rain samples collected from March 2014 to April 2015 from the northern coast (Erdemli,
91 Turkey) of the Levantine Basin, Eastern Mediterranean.

92

93 **2. Material and Methods**

94 **2.1. Sampling Site Description**

95 Aerosol and rain sampling were carried out at a rural site located on the coast of the
96 Eastern Mediterranean, Erdemli, Turkey (36° 33' 54" N and 34° 15' 18" E). The sampling tower
97 (above sea level ~ 22 m, ~ 10 m away from the sea) is situated at the Institute of Marine
98 Sciences, Middle East Technical University (IMS-METU). Its immediate vicinity is
99 surrounded by cultivated land to the north and to the south of the Northern Levantine Basin.
100 Although the site is not under the direct influence of any industrial activities (soda and
101 fertilizer), the city of Mersin with a population of 800.000 is located 45 km to the east of the
102 sampling site (Kubilay and Saydam, 1995; Koçak et al., 2012) and hence aerosol and
103 rainwater samples influenced by air mass transport from the east may have been influenced by
104 these regional anthropogenic activities.

105

106 **2.2. Sample Collection and Preparation**

107 *Aerosol*: A Gent type stacked filter unit (SFU) was used to collect aerosol samples in two size
108 fraction (coarse: $d = 10\text{-}2.5\ \mu\text{m}$ and fine: $d < 2.5\ \mu\text{m}$) (for more details see Hopke et al., 1997;
109 Koçak et al., 2007). Briefly, the first section of the filter holder was loaded with an 8 μm pore



110 size polycarbonate filter (Whatman Track Etched 111114, circle diameter: 47 mm), whilst the
111 second section was loaded with a 0.4 μm pore size polycarbonate filter (Whatman Track
112 Etched 111107, circle diameter: 47 mm). The cassette unit was then placed into the
113 cylindrical cassette holder, which is designed to prevent the intrusion of particles larger than
114 10 μm when the sampler is operated at a flow rate of 16.0-16.5 L/min. Daily (24 hours)
115 temporal sample resolution was carried out. Operational blank filters were processed in the
116 same way as the collected samples with the exception that no air was passed through the
117 filters. In order to minimize any possible contamination, the filter loading and unloading were
118 achieved in a laminar airflow cabinet.

119 The aerosol sampling campaign commenced in March 2014 and ended in April 2015.
120 During the sampling period, a total of 674 aerosol samples in two size fractions (coarse = 337;
121 fine = 337) were obtained. The observational coverage of the aerosol sampling period was 80
122 %. The sampling was terminated from time to time due to technical malfunction of the SFU
123 and/or cleaning procedure of sampling apparatus.

124

125 *Rain:* Rainwater samples were collected using an automatic Wet/Dry sampler (Model ARS
126 1000, MTX Italy). A total of 23 rain samples were collected during the sampling period. After
127 each rain event, the rainwater samples were immediately transferred to the laboratory for
128 filtration (0.4 μm Whatman, polycarbonate filters).

129

130 *Storage of Samples:* Aerosol and rainwater samples were stored frozen ($-20\text{ }^{\circ}\text{C}$) immediately
131 after collection until analyses (not more than a month). Cape et al. (2001) have been shown
132 that there were no significant losses for inorganic and organic nitrogen during the storage
133 (freezing for 3 months) of rain samples with an added biocide.

134



135 *Sample Preparation:* In order to determine the concentrations of water-soluble nitrogen
136 species (WSTN, NO_3^- and NH_4^+) and major water-soluble ions (Cl^- , SO_4^{2-} , Na^+ , K^+ , Mg^{2+} ,
137 Ca^{2+}) in an aerosol sample, one quarter of the filter was extracted for 60 minutes in 20 mL of
138 ultra-pure water (18.2 Ωm) by mechanic shaking. About 100 μL chloroform (Merc 2444, 99.8
139 %) was added as a preservative to prevent biological activity after removing the filter
140 (Bardouki et al., 2003, Koçak et al., 2007). Before measuring the water-soluble species,
141 extracts were filtered with 0.4 μm pore size polycarbonate filters.

142

143 2.3. Chemical Analysis

144 *Water Soluble Total Nitrogen:* High Temperature catalytic oxidation (Torch Teledyne Tekmar
145 TOC/TN) was applied to determine the WSTN concentrations in the aerosol and rainwater
146 samples. The liquid aliquot of the sample is injected into the combustion furnace (750 °C) and
147 the N in the sample was then converted to NO gas. The carrier gas (high purity dry air)
148 sweeps the sample into nondispersive infrared detector. From here, the sample is carried to
149 the nitrogen module. In this unit NO is mixed with O_3 since the chemiluminescent detection
150 of NO is based on the reaction between NO and O_3 . After the formation of excited nitrogen
151 dioxide (NO_2^*), the extra energy is given off as light when NO_2^* relaxes to its ground state.
152 The light signal to an electronic signal for quantification is then measured by a
153 chemiluminescence detector with a photomultiplier tube.

154

155 *Water soluble Inorganic and Ancillary Species:* In addition to NO_3^- and NH_4^+ , major water-
156 soluble ions concentrations were measured by using a Dionex ICS-5000 Ion Chromatography
157 instrument. Water-soluble anions (Cl^- , SO_4^{2-} , NO_3^-) were determined by applying AS11-HC
158 separation column, KOH (30 mM) eluent and AERS-500 (4 mm) suppressor whilst water-
159 soluble cations (Na^+ , K^+ , Mg^{2+} , Ca^{2+}) were detected electrochemically by using a CS12-A



160 separation column, MSA (20 mM) eluent and CSRS-300 (4 mm) suppressor (Product Manual
161 for Dionex IonPac AS11-HC-4m, IonPac CS12A Manual).

162 Blank values of WSTN for aerosol and rain samples were less than limit of detection
163 (20 ppb). The blank contributions of water-soluble ions in aerosol samples were found to be
164 less than 10 % and concentrations were corrected for blanks.

165

166 **2.4. Calculations**

167 WSON concentrations (see Eq. 1) were determined from the difference between the
168 individual concentrations of WSTN and water-soluble inorganic nitrogen (WSIN) (see Eq. 2)
169 since there is no direct analytical method to detect the concentration of water-soluble organic
170 nitrogen. The precision for WSON was calculated via using the formula (see Eq. 3) suggested
171 by Hansell (1993). The precision (75 nmol N m^{-3}) was found to be almost three times higher
172 (see Eq. 4, $R \sim 0.3$) than that of the arithmetic mean of WSON in aerosols whilst it ($90 \mu\text{mol N}$
173 L^{-1}) was estimated to be approximately four times larger than that of volume weighted mean
174 of WSON in rain. Such high values are not unusual. For example, if the data presented by
175 Mace et al. (2003a) would be used, precisions would have been 5 and 8 times higher
176 than those of the concentrations of WSON in aerosol and rain, respectively. Table 1 shows the
177 number of negative WSON values and the positive WSON biases for coarse and fine modes.
178 Correspondingly, about 5 (n=18) and 15 % (n=52) of the values were negative in coarse and
179 fine particles. The substitution with zero yielded 2 and 14 % positive bias for coarse and fine
180 mode whereas; the omission of zero resulted in 8 and 34 % positive bias in coarse and fine
181 WSON mean concentrations. Consequently, the presentation of the general characteristics of
182 the data includes all negative concentrations. In order to evaluate the variability in the aerosol
183 WSON and apply PMF, however, different approach was adopted. To this end, arbitrary
184 thresholds have been defined as the ratio between WSON mean concentration and the



185 calculated precision (see Eq. 4). Thus, during assessing the variability in aerosol WSON and
186 the application of PMF, WSON concentrations having R values larger than 0.3 will be
187 considered since the arbitrary threshold simply reduces the uncertainty.

$$WSON = WSTN - WSIN \quad (1)$$

$$WSIN = NO_3^- + NH_4^+ \quad (2)$$

$$S_{WSON} = (s_{WSTN}^2 + s_{WSIN}^2)^{1/2} \quad (3)$$

188

$$R = \frac{WSON_{MEAN}}{S_{WSON}} \quad (4)$$

189 The rain volume weighted average concentration (C_w) of nitrogen species can be
190 calculated as follow:

$$C_w = \frac{\sum_{i=1}^n C_i x Q_i}{\sum_{i=1}^n Q_i} \quad (5)$$

191 The wet and dry atmospheric fluxes of nitrogen species were calculated according to
192 the procedure explained in Herut et al. (1999, 2002). The wet atmospheric deposition fluxes
193 (F_w) were calculated from the annual precipitation (P_{annual}) and the volume weighted mean
194 concentration (C_w) of the substance of interest.

$$F_w = C_w \times P_{annual} \quad (6)$$

195 The dry deposition (F_d) is calculated as the product of the atmospheric mean nutrient
196 concentrations (C_d) and their settling velocities (V_d), where F_d is given in units of $\mu\text{mol m}^{-2}$
197 yr^{-1} , C_d in units of $\mu\text{mol m}^{-3}$ and V_d in units of m yr^{-1} .

$$F_d = C_d \times V_d \quad (7)$$

198 The settling velocities (V_d , see Eq. 8) for each water-soluble nitrogen species were
199 calculated by using an approach adopted by Spokes et al. (2001). C_c and C_f refer to as the
200 relative contribution of coarse and fine modes and 2.0 and 0.1 cm s^{-1} are deposition velocities
201 proposed by Duce et al. (1991) for coarse and fine particles respectively.



$$V_d = C_c \times 2.0 + C_f \times 0.1 \quad (8)$$

202

203 **2.5. Air Masses Back Trajectories and Airflow Classification**

204 Three day back trajectories of air masses at the four altitudes (1000, 2000, 3000 and
205 4000 meter) levels arriving at Erdemli station were computed by using the HYSPLIT
206 Dispersion Model (HybridSingle Particle Lagrangian Integrated Trajectory; Draxler and
207 Rolph, 2003). Three day back trajectories reaching at the altitude of 1000 m were classified
208 into six sectors: (i) Middle East, (ii) North Africa, (iii) Turkey, (iv) Eastern Europe, (v)
209 Western Europe and (vi) Mediterranean Sea in order to assess the influence of airflow on
210 WSON concentration in PM₁₀ (for more details see Koçak et al., 2012).

211

212 **2.6. Positive Matrix Factorization (PMF) for Source Apportionment of WSON**

213 The receptor modeling tool *Positive Matrix Factorization* (U.S. Environmental
214 Protection Agency PMF version 5.0, hereinafter referred to as ‘PMF’) was utilized to identify
215 the sources of WSON in PM₁₀ at Erdemli. PMF has been proven to be a robust tool in
216 characterizing the sources of aerosol (Paatero and Tapper, 1994; Huang et al., 1999; Lee et
217 al., 1999; Viana et al., 2008; Koçak et al., 2009). EPA PMF 5.0 software mainly consists of
218 Model Run and Rotational tools (see EPA/600/R-14/108; USEPA, 2014). Before application
219 of the software, the user must supply two input files namely, concentration and uncertainty.
220 The former contains concentrations of the aerosol species whilst the later has corresponding
221 uncertainty for each variable. Uncertainty was set to 5 % for each species with the exception
222 of WSON (15 %) since WSON exclusively donated high uncertainty. The base run of PMF
223 was achieved by setting the number of runs and random starting points (in other word seeds)
224 to 250 and 50, respectively. Base Model Displacement (DISP), Bootstrap (BS) and Bootstrap
225 Displacement (BS-DISP) methods were sequentially used after base run. The DISP accesses



226 the rotational ambiguity. DISP error estimates showed that there were no factor swaps and
227 significant decrease in Q during DISP, being 0 and 0.00, respectively. Therefore, DISP results
228 did not reveal rotational ambiguity, implying the solutions to be robust. Except in one case,
229 results from BS and BS-DISP (n=50) did not indicate any asymmetry and rotational
230 ambiguity for 5 factors. To evaluate the rotational ambiguity, different Fpeak values were
231 applied, considering changes in dQ to be less than 5 %. Furthermore, G-sape plots of Fpeak
232 solutions were examined to determine convergence toward the axis or lower/zero
233 contribution. Thus, Fpeak values of -0.7 was used and five factors were identified by using
234 PMF 5.0. BS of Fpeak at -0.7 did not reveal any swaps for five factors. The slope of the
235 estimated WSON against measured WSON was 10 % less than unity with correlation
236 coefficient and intercept of 0.87 and 1.5 (nmol N m⁻³), respectively.

237

238 3. Results and Discussion

239 3.1. General Characteristics of the Data

240 In this section the general characteristics of the Water-Soluble Organic Nitrogen
241 (WSON), Nitrate (NO₃⁻), Ammonium (NH₄⁺) and Water-Soluble Total Nitrogen (WSTN) in
242 aerosol and rain will be discussed.

243

244 *Aerosol:* The statistical summary for WSON, NO₃⁻, NH₄⁺ and WSTN in PM₁₀ aerosol
245 samples obtained from Erdemli between March 2014 and April 2015 is presented in Table 2.
246 Among the nitrogen species, WSON exhibited the highest arithmetic mean, followed by
247 ammonium and nitrate concentrations respectively. The maximum concentration of WSON
248 was estimated to be 79 nmol N m⁻³ with a mean value and standard deviation of 23.8 ± 16.3
249 nmol N m⁻³. Approximately 66 % of the WSON was associated with coarse particles, the
250 remaining fraction (34 %) was present within the fine mode. A number of studies have



251 reported the relative size distribution of WSON for the Eastern Mediterranean marine aerosol
252 (Finokalia, Violaki and Mihalopoulos, 2010) and those observed at remote marine sites
253 (Hawaii, Cornell et al., 2001; Tasmania, Mace et al., 2003a). The aerosol WSON at Finokalia
254 (68 %) and Hawaii were primarily found in the fine mode whilst WSON in the south Pacific
255 marine aerosol (Tasmania) it was mainly associated with the coarse fraction. It is likely that
256 the WSON at Erdemli (a) is relatively less impacted by anthropogenic sources and/or (b) is
257 more influenced by mineral dust transport and resuspension of cultivated soil compared to
258 that observed at Finokalia.

259 NO_3^- and NH_4^+ aerosol concentrations ranged between 0.2-88.4 and 0.5-164.4 nmol N m^{-3}
260 m^{-3} with mean values (standard deviations) of 17.9 (± 15.7) and 23.3 (± 24.4) nmol N m^{-3} . As
261 expected, NO_3^- was mainly associated with coarse particles, accounting for 87 % of the
262 observed mean value whilst NH_4^+ was dominant in the by fine mode, contributing 96 % to
263 the detected mean concentration. Similar results have been reported for Eastern
264 Mediterranean marine aerosol (Bardouki et al, 2003; Koçak et al., 2007). The predominance
265 of NO_3^- in the coarse mode might be due to gaseous nitric acid or other nitrogen oxides
266 reacting with alkaline sea salts and mineral dust particles. In contrast the occurrence of NH_4^+
267 in the fine fraction is mainly as a result of the reaction between gaseous alkaline ammonia and
268 acidic sulfuric acid (Mihalopoulos et al., 2007).

269 WSTN concentrations in aerosols varied between 9.7 and 176.5 nmol N m^{-3} with
270 arithmetic mean value of 63.5 ± 32.0 nmol N m^{-3} , respectively. The mean WSTN
271 concentration being almost equally influenced by coarse (51 %) and fine particles (49
272 %). Table 2 demonstrates the relative contributions of WSON, NO_3^- and NH_4^+ to the WSTN in
273 PM_{10} . As can be deduced from the table, the WSTN concentration was equally influenced by
274 WSON and NH_4^+ , each species contributing 37% and 35 %, respectively. In contrast the
275 contribution of NO_3^- to WSTN was found to be 28 %.



276

277 **Rain:** Volume-weighted-mean (VWM) concentrations of WSON, NO_3^- , NH_4^+ and WSTN in
278 rainwater are presented in Table 2, along with the minimum and maximum concentrations as
279 well as the relative contributions of WSON, NO_3^- and NH_4^+ to WSTN. As can be deduced
280 from table, VWM concentrations of each species were comparable, NH_4^+ exhibited the highest
281 concentration with a value of $28.7 \mu\text{mol N L}^{-1}$. The VWM concentration of WSON and NO_3^-
282 were 21.5 and $23.3 \mu\text{mol N L}^{-1}$, respectively. Considering their relative contributions to
283 WSTN, WSON and NO_3^- account 29 and 32 % of the WSTN whilst NH_4^+ represented 39 % of
284 the observed WSTN concentration in rainwater.

285

286 3.2. Comparison of WSON in Aerosol and Rain with data from the Literature

287 The concentrations of WSON in marine aerosols and rain samples collected from
288 different sites located around the Mediterranean, Atlantic and Pacific regions are illustrated in
289 Table 3. Comparing the current WSON values with those reported in the literature is
290 challenging due to (i) different applied sampling periods, sampling and measurement
291 techniques and (ii) the high uncertainty associated with the estimation of WSON.
292 Furthermore, within the literature there is a lack of information defining the uncertainty of
293 WSON though there is a substantial statistical knowledge. Keene et al. (2002) in particular,
294 have highlighted the tendency in the literature to neglect negative values or substitute such
295 values with zero instead when calculating the WSON from the difference between WSTN
296 and WSIN. As these authors have highlighted the omission or substitution of such values
297 inevitably would result in a positive bias in the WSON concentrations.

298 In general the lowest concentrations in aerosols were found in those derived from
299 remote or pristine marine environments. The WSON concentrations in the atmosphere over
300 the Indian (Amsterdam Island: $1.0 \text{ nmol N m}^{-3}$, Violaki et al., 2015), Atlantic (Barbados: 1.3



301 nmol N m^{-3} , Zamora et al., 2011) and Pacific Ocean (Hawaii, Oahu: $4.1 \text{ nmol N m}^{-3}$, Cornell
302 et al., 2001, Tasmania: $5.3 \text{ nmol N m}^{-3}$, Mace et al., 2003b) were at least 4 times less than
303 those observed for Eastern Mediterranean (Erdemli: $23.8 \text{ nmol N m}^{-3}$, this study; Finokalia:
304 $17.1 \text{ nmol N m}^{-3}$, Violaki and Mihalopoulos, 2010). These lower values might be attributed to
305 (i) the absence of the strong anthropogenic sources in the vicinity of the sampling sites and/or
306 (ii) the dilution of the WSON originating from long range transport via both dry and wet
307 deposition. The highest WSON concentrations emerged particularly over China (Ho et al.,
308 2015, concentration of WSON measured in $\text{PM}_{2.5}$) and Taiwan (Chen et al., 2010) with values
309 above 70 nmol N m^{-3} . As stated in Chen et al. (2010) WSON concentrations at these sampling
310 sites were markedly influenced by anthropogenic activities such as fossil fuel combustion and
311 man induced biomass burning. Concentrations over the Amazon (Mace et al., 2003c) in the
312 dry season (61 nmol N m^{-3}) have also been noted. Such high values were ascribed to natural
313 fires (Mace et al., 2003c). The mean WSON concentration at Erdemli ($23.8 \text{ nmol N m}^{-3}$) was
314 comparable to that reported previously for the same site (29 nmol N m^{-3} , Mace et al., 2003a).
315 In contrast, the present WSON concentration was almost 1.5 times higher than that observed
316 at Finokalia (Violaki and Mihalopoulos, 2010).

317 The reported WSON values for rain also exhibited the lowest concentrations in those
318 derived from remote or pristine marine environments, such as Hawaii ($2.8 \mu\text{mol N L}^{-1}$,
319 Cornell et al., 2001). The highest WSON concentrations were observed in China (North China
320 Plain: $103 \mu\text{mol N L}^{-1}$, Zhang et al., 2008) and Norwich, UK ($33 \mu\text{mol N L}^{-1}$, Cornell et al.,
321 1998), respectively. These high values were again attributed to the anthropogenic sources.

322

323 3.3. Temporal Variability of Water-Soluble Nitrogen Species in Aerosol Erdemli

324 Fig.1 illustrates daily variation of the water-soluble nitrogen species in aerosol
325 samples together with the daily rainfall from March 2014 to April 2015. The same figure also



326 presents the concentrations in rainwater samples collected between October 2014 and April
327 2015. It is clear that WSON concentrations exhibited large variations from one day to another
328 day. The daily variability in the concentration of WSON may be an order of magnitude. Such
329 variability has also been reported in the Atlantic (Zamora et al., 2011), Pacific (Chen et al.,
330 2010) and Eastern Mediterranean marine aerosols (Violaki and Mihalopoulos, 2010). These
331 studies demonstrated that the daily change in the concentrations of WSON arises from a
332 combination of (a) meteorological parameters (such as rain, temperature and wind
333 speed/direction), (b) chemical reactions, (c) history of air masses back trajectories and (d)
334 source emission strength.

335 In general, lower concentrations of WSON were found to be associated with rainy
336 days. To serve as an illustration, one of the lowest WSON concentrations was observed on
337 19th of October 2014, after two consecutive days of rainfall, with a value of 6 nmol N m^{-3} . In
338 contrast, one of the highest observed WSON concentrations ($66.1 \text{ nmol N m}^{-3}$) was detected
339 on 2nd of March 2014 when the air mass back trajectories were associated with south/south
340 westerly airflow (for more details see section 3.4). Another high concentration of WSON was
341 observed on 5th of July 2014, with a value 66 nmol N m^{-3} . 94% of the WSON was present in
342 the coarse mode, however, during this event there was no intense dust intrusion either from
343 the Sahara or from the Middle Eastern deserts. Corresponding OMI-AI index and nssCa^{2+} (33
344 nmol m^{-3}) also supports this observation (see Fig.2). Lower layer air mass back trajectories
345 (1000 and 2000 m) demonstrated that Erdemli was under the influence of north/north westerly
346 airflow from Turkey after passing over Turkey's largest cultivated plain, Konya. Thus, this
347 high value might be attributed to re-suspension of the soil affected by intense agricultural
348 activities. On 20th of January 2016 the WSON concentration was 60 nmol N m^{-3} , 72 % being
349 present in the fine mode. For this event, the NH_4^+ concentration was 20 nmol N m^{-3} , two
350 times higher than the observed arithmetic mean in winter. Corresponding trajectories, AOD



351 (Aerosol Optical Depth) and AC (Angstrom Component) images are presented in Fig.3.
352 Airflow at 1 km showed air mass flow arriving at the sampling site from Turkey. AOD values
353 over the sampling site and coastline of Northeastern Mediterranean ranged from 0.2 to 0.5
354 whilst AC values demonstrated that the region was dominated by fine particles. Based on
355 above indicators, it may be concluded that anthropogenic sources were dominant.

356 A summary of the statistical analyses of the seasonal dataset of aerosol associated
357 WSON, NO_3^- and NH_4^+ are shown in Table 4. The Mann-Whitney U test indicated that there
358 was a statistically significant difference among seasons, such that Summer > Spring \approx Winter
359 > Fall. The arithmetic mean value of WSON in the summer was found to be 1.3 and 2.0 times
360 greater those observed for Spring/Winter and Fall, respectively. Furthermore, WSON was
361 chiefly associated with coarse particles in summer, amounting to in excess of 80%. This high
362 value in summer might be due to the absence of rainfall (see Fig.1) and enhanced re-
363 suspension of cultivated soil in the region. In summer, the mean concentration of NH_4^+ was
364 almost 2.4 times larger than all other seasons. The mean water-soluble NO_3^- in summer was
365 1.4 high than that of spring. High NH_4^+ and NO_3^- concentrations in summer might be
366 attributed again to the absence of rainfall and increase in incoming radiation. Similar results
367 have been reported for the Eastern Mediterranean (Bardouki et al., 2003).

368

369 **3.4. Influence of Mineral Dust Episodes on WSON aerosol concentrations**

370 As it is well documented, the Eastern Mediterranean Sea is heavily impacted by
371 mineral dust episodes originating from Sahara and the Middle East deserts (Kubilay and
372 Saydam, 1995; Kubilay et al., 2000, Koçak et al., 2004a, b and 2012).

373

374 For the current study between March 2014 and April 2015, water-soluble non-sea salt calcium
375 concentrations higher than 50 nmol m^{-3} (2000 ng m^{-3} , as a threshold value) were defined as



376 mineral “dust events”. These events were additionally confirmed using air mass back
377 trajectories and OMI-AI. However, it is worth mentioning that for samples containing
378 concentrations of nssCa^{2+} less than 50 nmol m^{-3} mineral dust transport from Sahara and the
379 Middle East deserts to sampling site may not be excluded, peculiarly in winter. Yet, the
380 application of such an arbitrary value is inevitable since it provides simplicity to explore if
381 there is any influence of mineral dust intrusion on WSON.

382 For example, one of the highest WSON concentrations ($66.1 \text{ nmol N m}^{-3}$) was
383 observed on 2nd of March 2014 when the air mass back trajectories was associated with
384 south/south westerly airflow. During this event, nssCa^{2+} and NO_3^- showed a dramatic increase
385 in their concentrations compared to those observed during the previous day, reaching up to
386 429 and 60 nmol m^{-3} , respectively. OMI (Ozone Mapping Instrument) Aerosol Index (AI)
387 and three-day backward trajectory (1, 2, 3 and 4 km altitudes) air masses arriving at the
388 Erdemli sampling site on 2nd of March 2014 is shown in Fig.4. As can be seen from the figure,
389 all air masses (except at 1 km altitude) originated from North Africa whereas the back
390 trajectory for 1 km altitude exhibited airflow from the Middle East. Hence, suggesting that the
391 sampling site was under the influence of mineral dust transport originating from deserts
392 regions located at the Middle East and North Africa.. In support, the OMI-AI diagram clearly
393 indicates a large dust plume over the Eastern Mediterranean between coordinates 20-45 °N
394 and 15-40 °E. The Aerosol Index was found to be very high over the Northeastern
395 Mediterranean, ranging from 2.0 to 4.5. During this dust episode, 85% of the WSON was
396 associated with the coarse fraction, which further supports mineral dust being a main source
397 of water-soluble organic nitrogen.

398 Arithmetic mean concentrations together with corresponding standard deviations of
399 WSON, NO_3^- , NH_4^+ and nssCa^{2+} for dust and non-dust events are presented in Fig.5. As can
400 be deduced from diagram, (except for NH_4^+), WSON, NO_3^- and nssCa^{2+} indicated distinct



401 difference between dust and non-dust events. Indeed, the application of the non-parametric
402 Mann Whitney U test indicated statistically significant differences between dust and non-dust
403 events for WSON ($p < 0.03$), NO_3^- ($p < 0.00002$) and nssCa^{2+} ($p < 0.000001$) whereas no
404 statistically significant difference were observed for NH_4^+ ($p=0.56$). The crustally derived
405 nssCa^{2+} and anthropically derived NO_3^- for dust events had arithmetic mean of 95.8 nmol m^{-3}
406 and $26.1 \text{ nmol N m}^{-3}$ which were almost four and two times higher than those of observed for
407 non-dust events, respectively. Such an increase in concentrations during dust events for these
408 species has been previously reported in the Eastern Mediterranean (Koçak et al., 2004b).
409 Similarly, the arithmetic mean of WSON (38.2 nmol m^{-3}) during dust events was 1.3 times
410 higher compared to the value observed during non-dust events (29.4 nmol m^{-3}). A similar
411 enrichment of WSON during dust events has been reported for Erdemli (Mace et al., 2003a;
412 Yellow Sea (Shi et al., 210) and Finokalia (Violaki and Mihalopoulos, 2010). In addition,
413 Griffin et al. (2007) have demonstrated a significant difference between dust and non-dust
414 events for bacterial and fungal colony forming units at Erdemli, the former being much
415 greater.. Thus, it might be speculated that this enhancement during dust events can be due to
416 (a) mineral dust borne microorganisms and/or (b) interaction (e.g. adsorption, acid-base
417 reaction) between mineral dust and organic nitrogen compounds.

418

419 3.5. Impact of Airflow on WSON

420 Arithmetic mean concentrations together with corresponding standard deviations for water-
421 soluble nitrogen species and nssCa^{2+} in aerosol samples according to categorized air mass
422 sectors (at 1 km) are presented in Table 5 WSON concentrations can be broadly categorized
423 in two classes namely (a) Middle East, North Africa, Turkey and (b) Eastern Europe, Western
424 Europe and Mediterranean Sea. WSON concentrations in the first group were found to be at
425 least 1.2 higher than those observed for the second group. The application of the Mann-



426 Whitney U test indicated that there was a statistically significant difference in the
427 concentrations of WSON between the following air mass categories: North
428 Africa/Turkey/Middle East > Eastern Europe/Western Europe/ Mediterranean Sea ($p < 0.05$)
429 The highest NO_3^- concentrations were associated with airflow from North Africa and Turkey
430 with value of 18 and 15 nmol N m^{-3} , respectively, and there was a statistically significant
431 difference compared to the remaining air mass sectors ($p > 0.05$). The mean concentrations of
432 NO_3^- for air masses derived from North Africa and Turkey was at least 1.3 times larger than
433 those calculated for the Middle East, Eastern Europe, Western Europe and Mediterranean Sea
434 air sectors ($p > 0.05$). NH_4^+ had the highest concentration under the influence of airflow
435 derived from Turkey. For this airflow, detected concentration was 1.5-2.4 times greater than
436 those calculated for other air masses sectors. The Mann-Whitney test showed that there was a
437 statistically significant difference in the nssCa^{2+} concentrations. Arithmetic mean
438 concentrations of nssCa^{2+} in the Middle East and North Africa were approximately 2 times
439 higher compared to the remaining air masses. As expected, these two airflows were primarily
440 influenced by crustal material due to sporadic dust events originating from deserts located in
441 North Africa and the Middle East.

442

443 3.6. Source Apportionment for WSON in Aerosol

444 A number of studies have discussed the possible sources of WSON in aerosol material
445 by applying either simple correlation analyses (Mace et al., 2003c; Violaki and Mihapoulos,
446 2010; Ho et al., 2015) or multivariate factor analysis (Chen and Chen, 2010), including PMF
447 (Chen et al., 2010). Usage of correlation analyses is useful when the number in sample-
448 populations are limited however; large datasets are required in order to carry out PMF and FA.
449 Direct and indirect emissions of WSON from the sea surface have been demonstrated
450 (Miyakazi et al., 2011; Altieri et al., 2016). Previous studies in the Eastern Mediterranean,



451 have observed WSON to be associated with mineral dust (Mace et al., 2003a; Violaki and
452 Mihalopoulos, 2010). As stated by Mace et al. (2003a), WSON might either have originated
453 from mineral dust or carried by dust events owing to adsorption of gaseous organic nitrogen
454 compounds onto pre-existing particles. In addition, Violaki and Mihalopoulos (2010) have
455 shown fossil fuel and biomass burning as sources of WSON to the Eastern Mediterranean
456 atmosphere.

457 Fig.6 describes the potential sources of WSON by applying PMF 5.0. The
458 predominant two factors were chiefly found to be related with water-soluble inorganic
459 nitrogen species. The first factor had a high-loading for NH_4^+ with a value of 0.81 and a
460 moderate loading of SO_4^{2-} (0.45). These species, would suggest the formation of secondary
461 aerosols. As expected, the factor contribution plot (not shown) indicated summer maximum,
462 demonstrating accumulation of these particles due to the absence of rain and enhanced gas-to-
463 particle formation under the prevailing conditions (high temperature and solar radiation). The
464 equivalent ratio of NH_4^+ and SO_4^{2-} for this factor was 0.79, indicating $(\text{NH}_4)\text{HSO}_4$
465 formation (Koçak et al., 2007). The second factor explained 77 % of the NO_3^- variation and
466 described 17 and 10 % of the SO_4^{2-} and NH_4^+ , variation, respectively. This group was also
467 associated with cations such as Na^+ (11 %), K^+ (7 %), Mg^{2+} (22 %) and Ca^{2+} (29 %), implying
468 reactions mainly between acidic nitrate and alkaline species. The first and second factors
469 accounted for 20 and 22 % of the variability in WSON, respectively. It might, therefore be
470 argued that the variability of WSON in the first group resulted from the reaction between
471 volatile organic N and ammonium sulfate aerosols whilst the variability of WSON explained
472 by the second factor was as a result of the reaction between volatile organic compounds and
473 NO_x and/or neutralization of acidic nitrate by alkaline nitrogen-containing compounds such as
474 urea and amine. The third factor was heavily influenced by Cl^- (0.8) and Na^+ (0.70) while
475 moderately impacted by Mg^{2+} and K^+ . This factor is likely due to sea salt formation. The



476 forth factor was predominantly impacted by Ca^{2+} and hence may be attributed to crustal
477 material. Crustal sources explained 10 % of the WSON variability. The final defined factor
478 had a moderate loading of WSON ($\text{EV} = 0.43$, explained 43 %) while it was affiliated with
479 Na^+ (0.15), K^+ (0.22) and Mg^{2+} (0.24). The factor contribution diagram denoted highest
480 values in summer (not shown) and hence it can be attributed to re-suspension of the soil
481 particularly affected by intense agricultural activities.

482

483 **3.7. Atmospheric Depositions of N-Species and Implications Regarding Marine** 484 **Production**

485 The atmospheric dry ($21.3 \text{ mmol N m}^{-2} \text{ yr}^{-1}$) and wet ($36.7 \text{ mmol N m}^{-2} \text{ yr}^{-1}$)
486 deposition fluxes of WSON, NO_3^- and NH_4^+ and WSTN from March 2014 and April 2015
487 are demonstrated in Table 6. The atmospheric deposition of water-soluble nitrogen (57.8 mmol
488 $\text{N m}^{-2} \text{ yr}^{-1}$) was chiefly originated from wet deposition ($36.7 \text{ mmol N m}^{-2} \text{ yr}^{-1}$), amounting to
489 63 % of the total atmospheric deposition. This difference might be attributed to the water-
490 soluble ammonium, for instance, the atmospheric depositions of NH_4^+ ($15.6 \text{ mmol N m}^{-2} \text{ yr}^{-1}$)
491 was dominated by wet deposition, contributing 92 % of the total ammonium atmospheric flux.
492 Whereas, the atmospheric flux of WSON and NO_3^- were more or less equally influenced by
493 both deposition modes. Corresponding WSON ($9.8 \text{ mmol N m}^{-2} \text{ yr}^{-1}$) and NO_3^- (10.0 mmol N
494 $\text{m}^{-2} \text{ yr}^{-1}$) contributions to dry deposition were found to be 46 % and 48 % respectively. In
495 contrast, NH_4^+ ($1.3 \text{ mmol N m}^{-2} \text{ yr}^{-1}$) was only estimated to contribute 6 % of the total
496 deposition. Wet deposition of nitrogen was impacted by WSON ($10.8 \text{ mmol N m}^{-2} \text{ yr}^{-1}$), NO_3^-
497 ($11.7 \text{ mmol N m}^{-2} \text{ yr}^{-1}$), and NH_4^+ ($14.3 \text{ mmol N m}^{-2} \text{ yr}^{-1}$) in the increasing order 29 % < 32 %
498 < 39 %. On average, WSON accounted for 36 % of the total atmospheric deposition of
499 WSTN.



500 If one assumes that all N species are bioavailable to primary producers for primary
501 production and if a Redfield N/C ratio of 106/16 is applied, it would be estimated that
502 atmospheric N depositions can support new production 7.95 g C yr^{-1} . It has been shown that
503 annual primary production for coastal and open waters of Cilician Basin were around 413 mg
504 $\text{C m}^{-2} \text{ d}^{-1}$ and $179 \text{ mg C m}^{-2} \text{ d}^{-1}$, respectively (Yücel, 2013). It has been noted that f- ratio
505 (ratio between new and total production) may ranged between 0.05 and 0.16 in oligotrophic
506 seas such as Mediterranean (Estrada, 1996 and references therein). If the f-ratio of 0.16 is
507 applied, the annual new production for coastal and open waters of Cilician Basin would be
508 $24.15 \text{ g C yr}^{-1}$ and 10.5 g C yr^{-1} respectively. Consequently, the atmospheric water-soluble
509 nitrogen flux was found to sustain 33 % of the new production in coastal and 76 % of it in
510 open waters.

511

512 **4. Conclusion**

513 In the current study, water-soluble organic nitrogen in aerosol and rain samples
514 obtained over the Eastern Mediterranean has been investigated. From this investigation the
515 following summary may be made:

516 1) Of the nitrogen species, aerosol WSON ($23.8 \pm 16.3 \text{ nmol N m}^{-3}$) exhibited the
517 highest arithmetic mean, followed by ammonium ($23.3 \pm 14.4 \text{ nmol N m}^{-3}$) and then nitrate
518 ($17.9 \pm 15.7 \text{ nmol N m}^{-3}$). Aerosol WSON was mainly associated with coarse particles (66
519 %). The WSTN was equally influenced by WSON and NH_4^+ , each contributing 37 and 35 %,
520 respectively, whereas the contribution to WSTN of NO_3^- was 28 %. In rainwater, the VWM
521 concentrations of water-soluble nitrogen species were comparable. WSON and NO_3^-
522 accounted for 29 and 32 % of the WSTN whilst NH_4^+ elucidated 39 % of the WSTN.

523 2) Aerosol WSON concentrations exhibited large variations from one day to another
524 day. Generally, lower concentrations were observed during rainy days. Higher concentrations



525 of aerosol WSON were associated with different airflow. The three highest concentrations
526 were related to (i) mineral dust transport from Sahara and the Middle East deserts, (ii)
527 north/north westerly airflow from Turkey's largest cultivated plain, Konya and (iii) mid-range
528 pollution transport from the Turkish coast. 3) Influence of mineral dust transport on aerosol
529 WSON concentrations was assessed. The crustally derived Ca^{2+} and anthropogenic NO_3^-
530 for dust events had arithmetic mean of 95.8 nmol m^{-3} and $26.1 \text{ nmol N m}^{-3}$ which were almost
531 four and two times higher than those of observed for non-dust events. The arithmetic mean of
532 WSON (38.2 nmol m^{-3}) for dust events was 1.3 times higher compared to that observed for
533 non-dust events (29.4 nmol m^{-3}).

534 4) Source apportionment suggested that aerosol WSON was mainly originated from
535 anthropogenic sources including agricultural (43 %), secondary aerosols (20 %) and nitrate
536 (22%), whereas, the two natural sources crustal material (10 %) and sea salts (5%) contributed
537 15 % to the WSON.

538 5) The total atmospheric deposition of water-soluble nitrogen ($57.8 \text{ mmol N m}^{-2} \text{ yr}^{-1}$)
539 ¹) was mainly via wet deposition ($36.7 \text{ mmol N m}^{-2} \text{ yr}^{-1}$). In contrast the atmospheric fluxes of
540 WSON and NO_3^- were equally influenced by the dry and wet deposition modes. On average,
541 WSON accounted for 36 % of the total atmospheric deposition of WSTN. The annual new
542 production for coastal and open waters of Cilician Basin was estimated to be $24.15 \text{ g C yr}^{-1}$
543 and 10.5 g C yr^{-1} , respectively. Using these estimates the atmospheric water-soluble nitrogen
544 flux could sustain 33 % of the new production in coastal and 76 % of it in open waters.

545

546

547

548

549



550 The authors declare that they have no conflict of interest.

551 **Acknowledgments**

552 This work was mainly supported by The Scientific and Technological Research Council of
553 Turkey (TUBITAK). Required data were collected within the framework of the TUBITAK
554 113Y107 project. This study was also supported by the DEKOSIM (Center for Marine
555 Ecosystem and Climate Research) Project (BAP-08-11-DPT.2012K120880) funded by
556 Ministry of Development of Turkey. We would like to thank to Ersin Tursak, Pınar Kalegeri
557 and Merve Açıkıyol for helping during sample collection and analysis. Aerosol optical
558 thickness, angstrom component and aerosol index values used in this study were produced
559 with the Giovanni online data system, developed and maintained by the NASA GES DISC.
560 We also acknowledge the MODIS and OMI mission scientists and associated NASA
561 personnel for the production of the data used in this research effort.

562

563 M. Koçak developed the concept and designed the study. M. Nehir and M. Koçak performed
564 the experiments, analyzed the data and prepared the manuscript.

565

566 **References**

- 567 Altieri, K., Fawcett, S., Peters, A., Sigman, D., Hastings, M.: Marine biogenic source
568 of atmospheric organic nitrogen in the subtropical North Atlantic. *P. Natl. Acad. Sci.*, *113* (4),
569 925-930, 2016.
- 570 Bardouki, H., Liakakou, H., Economou, C., Sciare, J., Smolik, J., Zdimal, V.,
571 Eleftheriadis, K., Lazaridis, M., Dye, C., Mihalopoulos, N.: Chemical composition of size
572 resolved atmospheric aerosols in the eastern Mediterranean during summer and winter. *Atmos.*
573 *Environ.*, *37*, 195–208, 2003.
- 574 Cape, J. N., Kirika, A., Rowland, A. P., Wilson, D. R., Jickells, T. D., Cornell, S:
575 Organic nitrogen in precipitation: real problem or sampling artefact? *The Scientific World*, *1*,
576 230–237, 2001.
- 577 Chen, H. and Chen, L.: Occurrence of water soluble organic nitrogen in aerosols at a
578 coastal area. *J. Atmos. Chem.*, *65*, 49–71, 2010, doi: 10.1007/s10874-010-9181-y.
- 579 Chen, H., Chen, L., Chiang, Z., Hung, C., Lin, F., Chou, W., Gong, G., Wen, L.: Size
580 fractionation and molecular composition of water-soluble inorganic and organic nitrogen in
581 aerosols of a coastal environment. *J. Geophys. Res.*, *115*, D22, 2010,
582 doi:10.1029/2010JD014157.
- 583 Cornell, S., Rendell, A. Jickells, T.: Atmospheric inputs of dissolved organic nitrogen
584 to the oceans, *Nature*, *376*, 243–246, 1995.
- 585 Cornell, S., Jickells T., Thornton C.: Urea in rainwater and atmospheric aerosol,
586 *Atmos. Environ.*, *32*, 1903-1910, 1998.
- 587 Cornell, S., Mace, K., Coeppicus, S., Duce, R., Huebert, B., Jickells, T., Zhuang, L.Z.:
588 Organic nitrogen in Hawaiian rain and aerosols. *J. Geophys. Res.* *106*, 7973–7983, 2001.
- 589 Cornell, S. E., Jickells, T. D., Cape, J. N., Rowland, A. P., Duce, R.A.: Organic
590 nitrogen deposition on land and coastal environments: a review of methods and data, *Atmos.*
591 *Environ.*, *37*, 2173–2191, 2003.
- 592 De Haan, D.O., Hawkins, L.N., Kononenko, J.A., Turley, J.J., Corrigan, A.L., Tolbert,
593 M.A., Jimenez, J.L.: Formation of Nitrogen-Containing Oligomers by Methylglyoxal and
594 Amines in Simulated Evaporating Cloud Droplets, *Environ. Sci. Technol.*, *45*, 948-991, 2011.
- 595 Draxler, R.R., Rolph, G.D., 2003. HYSPLIT (HYbrid Single-Particle Lagrangian
596 Integrated Trajectory), Model Access via NOAA ARL READY Website. NOAA Air
597 Resources Laboratory, Silver Spring, MD. <http://www.arl.noaa.gov/ready/hysplit4.html>.
- 598 Duce, R.A., Liss, P.S., Merrill, J.T., Atlas, E.L., Buat-Menard, P.: The atmospheric
599 input of trace species to the world ocean. *Glob. Biogeochem. Cycles*, *5*, 193–259, 1991.
- 600
- 601 Duce, R. A., LaRoche, J., Altieri, K., Arrigo, K. R., Baker, A. R., Capone, D. G.,
602 Cornell, S., Dentener, F., Galloway, J., Ganeshram, R. S., Geider, R. J., Jickells, T., Kuypers,
603 M. M., Langlois, R., Liss, P. S., Liu, S. M., Middelburg, J. J., Moore, C. M., Nickovic, S.,
604 Oschlies, A., Pedersen, T., Prospero, J., Schlitzer, R., Seitzinger, S., Sorensen, L. L.,



- 605 Uematsu, M., Ulloa, O., Voss, M., Ward, B., Zamora, L.: Impacts of atmospheric
606 anthropogenic nitrogen on the open ocean. *Science*, 320, 893–897, 2008.
- 607 Estrada, M.: Primary production in the northwestern Mediterranean. *Sci. Mar.*, 60 (2),
608 55–64, 1996.
- 609 Galloway, J., Cowling, E.: Reactive nitrogen and the world: 200 years of change.
610 *Ambio* 31, 64–71, 2002.
- 611 Galloway, J. N., Townsend, A. R., Erisman, J.W., Bekunda, M., Cai, Z. C., Freney, J.
612 R., Martinelli, L. A., Seitzinger, S. P., Sutton, M. A.: Transformation of the nitrogen cycle:
613 Recent trends, questions, and potential solutions, *Science*, 320, 889–892, 2008.
- 614 Galloway, M. M., Chhabra, P. S., Chan, A. W. H., Surratt, J. D., Flagan, R. C.,
615 Seinfeld, J. H., Keutsch, F. N.: Glyoxal uptake on ammonium sulphate seed aerosol: reaction
616 products and reversibility of uptake under dark and irradiated conditions. *Atmos. Chem. Phys.*,
617 9, 3331–3345, 2009. doi:10.5194/acp-9-3331-2009.
- 618 Ge, X., Wexler, A., Clegg, S., 2011. Atmospheric amines e part I. A review. *Atmos.*
619 *Environ.* 45, 524–546.
- 620 Glibert PM, Trice TM, Michael B, Lane L.: Urea in the tributaries of the Chesapeake
621 and coastal bays of Maryland. *Water Air Soil Poll.* 43, 160–229, 2005.
- 622 Griffin, D.W., Kubilay, N., Koçak, M., Gray, M.A., Borden, T.C., Shinn, E: Airborne
623 desert dust and aeromicrobiology over the Turkish Mediterranean coastline. *Atmos. Environ.*,
624 41, 4050–4062, 2007.
- 625 Hamad, N., Millot, C., Taupier-Letage, I.: A new hypothesis about the surface
626 circulation in the eastern basin of the Mediterranean Sea. *Prog. Oceanogr.*, 66, 287–298,
627 2005.
- 628 Hansell, D.: Results and observations from the measurement of DOC and DON in
629 seawater using a high-temperature catalytic oxidation technique. *Mar. Chem.*, 41, 195–202,
630 1993.
- 631 Herut, B., Krom, M.D., Pan, G., Mortimer, R.: Atmospheric input of nitrogen and
632 phosphorus to the Southeast Mediterranean: sources, fluxes, and possible impact. *Limnol.*
633 *Oceanogr.*, 44, 1683–1692, 1999.
- 634 Herut, B., Collier, R., Krom, M. D.: The role of dust in supplying nitrogen and
635 phosphorus to the Southeast Mediterranean. *Limnol. Oceanogr.*, 47, 870–878, 2002.
- 636 Ho, K., Ho, S. S., Huang, R., Liu, S., Cao, J., Zhang, T., Chuang H., Chan C.S., Hu D.,
637 Tian, L.: Characteristics of water-soluble organic nitrogen in fine particulate matter in the
638 continental area of China. *Atmos. Environ.*, 106, 252–261, 2014.
- 639
- 640 Hopke, P. K., Xie, Y., Raunemaa, T., Biegalski, S., Landsberger, S., Maenhaut, W.,
641 Artaxo, P., Cohen, D.: Characterization of the Gent Stacked Filter Unit PM₁₀ Sampler.
642 *Aerosol Sci. Tech.*, 27, 726–735, 1997.



- 643 Huang, S., Rahn, K.A., Arimoto, R.: Testing and optimizing two factor analysis
644 techniques on aerosol at Narragansett, Rhode Island. *Atmos. Environ.*, *33*, 2169–2185, 1999.
- 645 Keene, W., Montag, J., Maben, J., Southwell, M., Leonard, J., Church, T., Moody, J.,
646 Galloway, J.: Organic nitrogen in precipitation over Eastern North America. *Atmos. Environ.*,
647 *36*(28), 4529–4540, 2002.
- 648 Koçak M., Nimmo, M., Kubilay, N., Herut, B.: Spatio-temporal aerosol trace metal
649 concentrations and sources in the Levantine Basin of the Eastern Mediterranean. *Atmos.*
650 *Environ.*, *38*, 2133–2144, 2004a.
- 651 Koçak, M., Kubilay, N., Mihalopoulos, N.: Ionic composition of lower tropospheric
652 aerosols at a Northeastern Mediterranean site: implications regarding sources and long-range
653 transport. *Atmos. Environ.*, *38*, 2067–2077, 2004b.
- 654 Koçak, M., Mihalopoulos, N., Kubilay, N.: Chemical composition of the fine and
655 coarse fraction of aerosols in the Northeastern Mediterranean. *Atmos. Environ.*, *41*, 7351–
656 7368, 2007.
- 657 Koçak, M., Mihalopoulos, N., Kubilay, N.: Source regions of PM10 in the Eastern
658 Mediterranean atmosphere. *Atmos. Res.*, *92*, 464–474, 2009.
- 659 Koçak, M., Theodosi, C., Zarnpas, P., Seguret, M.J.M., Herut, B., Kallos, G.,
660 Mihalopoulos, N., Kubilay, N., Nimmo, M.: Influence of mineral dust transport on the
661 chemical composition and physical properties of the Eastern Mediterranean aerosol. *Atmos.*
662 *Environ.* *57*, 266–277, 2012.
- 663 Krom, M.D., Herut, B., Mantoura, R.F.C.: Nutrient budget for the Eastern
664 Mediterranean: implications for P limitation. *Limnol. Oceanogr.*, *49*, 1582–1592, 2004.
- 665 Kubilay, N. and Saydam, C.: Trace elements in atmospheric particulates over the
666 Eastern Mediterranean: concentration, sources and temporal variability. *Atmos. Environ.*, *29*,
667 2289–2300, 1995.
- 668 Kubilay N., Nickovic S., Moulin C., Dulac F.: An illustration of the transport and
669 deposition of mineral dust onto the eastern Mediterranean. *Atmos. Environ.*, *34*, 1293–1303,
670 2000.
- 671 Lee, E., Chan, C.K., Paatero, P.: Application of positive matrix factorization in source
672 apportionment of particulate pollutants in Hong Kong. *Atmos. Environ.*, *33*, 3201–3212, 1999.
- 673 Mace, K.A., Kubilay, N., Duce, R.A.: Organic nitrogen in rain and aerosol in the
674 eastern Mediterranean atmosphere: An association with atmospheric dust. *J. Geophys. Res.*,
675 *108*, D10, 4320, 2003a, doi:10.1029/2002JD002997.
- 676 Mace KA, Duce RA, Tindale NW.: Organic nitrogen in rain and aerosol at Cape Grim,
677 Tasmania Australia. *J. Geophys Res.*, *108*, 4338, 2003b.
- 678 Mace, K., Artaxo, P., Duce, R.: Water-soluble organic nitrogen in Amazon Basin
679 aerosols during the dry (biomass burning) and wet seasons. *J. Geophys. Res.* *108*, 4512,
680 2003c. <http://dx.doi.org/10.1029/2003JD003557>.
- 681 Mihalopoulos, N., Kerminen, V., M., Kanakidou, M., Berresheim, H., Sciare, J.:



- 682 Formation of particulate sulfur species (sulfate and methanesulfonate) during summer over
683 the Eastern Mediterranean: a modelling approach. *Atmos. Environ.* *41*, 6860–6871, 2007.
- 684 Miller, J.: The nitrogen content of rain falling at Rothamsted. *J. Agric. Sci.*, *1*, 280–
685 303, 1905.
- 686 Miyazaki, Y., Kawamura, K., Jung, J., Furutani, H., Uematsu, M.: Latitudinal
687 distributions of organic nitrogen and organic carbon in marine aerosols over the western
688 North Pacific, *Atmos. Chem. Phys.*, *11*, 3037–3049, 2011. doi:10.5194/acp-11-3037-2011.
- 689 Neff, J. C., Holland, E. A., Dentener, F. J., McDowell, W. H., and Russell, K. M.: The
690 origin, composition and rates of organic nitrogen deposition: A missing piece of the nitrogen
691 cycle. *Biogeochemistry*, *57*, 99–136, 2002.
- 692 Paatero, P., Tapper, U.: Positive matrix factorization: a non-negative factor model with
693 optimal utilization of error estimates of data value. *Environmetrics*, *5*, 111–126, 1994.
- 694 Peierls, B. L. and Paerl, H. W.: Bioavailability of atmospheric organic nitrogen
695 deposition to coastal phytoplankton. *Limnol. Oceanogr.*, *42*, 1819–1823, 1997.
- 696 Seitzinger, S. P. and Sanders, R. W.: Atmospheric inputs of dissolved organic nitrogen
697 stimulate estuarine bacteria and phytoplankton. *Limnol. Oceanogr.*, *44*, 721–730, 1999.
- 698 Shi, J.H., Gao, H.W., Qi, J.H., Zhang, J., Yao, X.H.: Sources, compositions, and
699 distributions of water-soluble organic nitrogen in aerosols over the China Sea. *J. Geophys.*
700 *Res.* *115*, 2010.
- 701 Sorooshian, A., Murphy, S. M., Hersey, S., Gates, H., Padro, L. T., Nenes, A.,
702 Brechtel, F. J., Jonsson, H., Flagan, R. C., Seinfeld, J. H.: Comprehensive airborne
703 characterization of aerosol from a major bovine source. *Atmos. Chem. Phys.*, *8* (17), 5489–
704 5520, 2008.
- 705 Spokes, L.J., Jickells, T. D., Jarvis, K.: Atmospheric inputs of trace metals to the
706 northeast Atlantic Ocean: the importance of south-easterly flow. *Mar. Chem.*, *76*, 319–330,
707 2001.
- 708 Surratt, J.D., Gómez-González, Y., Chan, A.W.H., Vermeylen, R., Shahgholi, M.,
709 Kleindienst, T.E., Edney, E.O., Offenberg, J.H., Lewandowski, M., Jaoui, M., Maenhaut,
710 Claeys, W.M., Flagan, R.C. and Seinfeld, J.H.: Organosulfate Formation in Biogenic
711 Secondary Organic Aerosol. *J. Phys. Chem. A*, *112* (36), 8345–8378, 2008.
- 712 Twohy, C. H., Petters, M. D., Snider, J. R., Stevens, B., Tahnk, W., Wetzal, M.,
713 Russell, L., Burnet, F.: Evaluation of the aerosol indirect effect in marine stratocumulus
714 clouds: Droplet number, size, liquid water path, and radiative impact. *J. Geophys. Res.*, *110*,
715 D08203, 2005. doi:10.1029/2004JD005116.
- 716
- 717 Thingstad, T. F., Krom, M. D., Mantoura, R. F. C., Flaten, G. A. F., Groom, S., Herut,
718 B., Kress, N., Law, C. S., Pasternak, A., Pitta, P., Psarra, S., Rassoulzadegan, F., Tanaka, T.,
719 Tselepidis, A., Wassmann, P., Woodward, E. M. S., Riser, C. Wexels, Zodiatis, G., Zohary,
720 T.: Nature of Phosphorus Limitation in the Ultraoligotrophic Eastern Mediterranean. *Science*,



- 721 309, 1068-1071, 2005.
- 722 Timperley MH, Vigor-Brown RJ, Kawashima M, Ishigami M.: Organic nitrogen
723 compounds in atmospheric precipitation: their chemistry and availability to phytoplankton.
724 *Canadian J. Fish Aquat. Sci.*, 42, 1171–1177, 1985.
- 725 Viana, M., Pandolfi, M., Minguillon, M.C., Querol, X., Alastuey, A., Monfort, E.,
726 Celades, I.: Inter-comparison of receptor models for PM sources apportionment: case study in
727 an industrial area. *Atmos. Environ.* 42, 3820–3832, 2008.
- 728 Violaki, K. and Mihalopoulos, N.: Water-soluble organic nitrogen (WSON) in size-
729 segregated atmospheric particles over the Eastern Mediterranean. *Atmos. Environ.*, 44, 4339-
730 4345, 2010.
- 731 Violaki, K., Zarbas, P., Mihalopoulos, N.: Long-term measurements of dissolved
732 organic nitrogen (DON) in atmospheric deposition in the Eastern Mediterranean: fluxes,
733 origin and biogeochemical implications. *Mar. Chem.* 120, 179-186, 2010.
- 734 Violaki, K., Sciare, J., Williams, J., Baker, A.R., Martino, M., Mihalopoulos, N.:
735 Atmospheric Water-Soluble Organic Nitrogen (WSON) over marine environments: A global
736 perspective. *Biogeosciences*, 12, 3131-3140, 2015.
- 737 Yılmaz, A. and Tuğrul, S.: The effect of cold- and warm-core eddies on the
738 distribution and stoichiometry of dissolved nutrients in the northeastern Mediterranean. *J.*
739 *Mar. Sys.*, 16, 253–268, 1998.
- 740 Yu, G., Bayer, A. R., Galloway, M. M., Korshavn, K. J., Fry, C. G., Keutsch, F. N.:
741 Glyoxal in Aqueous Ammonium Sulfate Solutions: Products, Kinetics and Hydration Effects.
742 *Environ. Sci. Tech.*, 45, 6336–6342, 2011. doi:10.1021/es200989n.
- 743 Yücel, N.: Monthly changes in primary and bacterial productivity in the north-eastern
744 Mediterranean shelf waters. *Ph.D. thesis*, Middle East Technical University, Institute of
745 Marine Sciences, Erdemli, Turkey, 2013.
- 746 Yücel, N.: Seasonal and spatial variation of bacterial production and abundance in the
747 northern Levantine Sea. *Mediterr. Mar. Sci.*, 18, 97-106, 2017.
- 748 Zamora, L. M., Prospero, J. M., Hansell, D. A.: Organic nitrogen in aerosols and
749 precipitation at Barbados and Miami: Implications regarding sources, transport and deposition
750 to the western subtropical North Atlantic. *J. Geophys. Res.*, 116, D20, 2011.
- 751 Zhang, Y., Zheng, L., Liu, X., Jickells, T., Cape, N., Goulding, K., Fangmeier, A. and
752 Zhang, F.: Evidence for organic N deposition and its anthropogenic sources in China. *Atmos.*
753 *Environ.*, 42, 1035-1041, 2008.
- 754
- 755
- 756
- 757
- 758



759 **Figure Captions**

760 **Figure 1.** The daily variations in the concentrations of (a) WSON, (b) NO_3^- and (c) NH_4^+
761 (nmol N m^{-3}) together with rain amount (mm) from March 2014 and April 2015 for PM10.

762 **Figure 2.** Three day back trajectories showing the transport of air masses 1000m (black
763 circle), 2000m (black star), 3000m (black square) and 4000m (black triangle) on 5th of July
764 2014 for Erdemli. Aerosol Index (AI) from OMI (Ozone Mapping Instrument) distribution
765 also illustrated with a color bar from grey to black.

766 **Figure 3.** Three day back trajectories showing the transport of air masses 1000m (black
767 circle), 2000m (black star), 3000m (black square) and 4000m (black triangle) on 20th of
768 February 2015 for Erdemli. Aerosol Optical Depth (AOD, a) and Angstrom Component (AC,
769 b) from MODIS (Moderate Resolution Imaging Spectroradiometer) distribution also
770 demonstrated with a color bar from grey to black.

771 **Figure 4.** Three day back trajectories indicating the transport of air masses 1000m (black
772 circle), 2000m (black star), 3000m (black square) and 4000m (black triangle) on 2nd of
773 March 2014 for Erdemli. Aerosol Index (AI) from OMI (Ozone Mapping Instrument)
774 distribution also illustrated with a color bar from grey to black.

775 **Figure 5.** Arithmetic means together with corresponding Standard deviations of WSON, NO_3^-
776 , NH_4^+ and nssCa^{2+} for dust and non-dust events at Erdemli site. Dark and light grey bars
777 denote arithmetic mean for dust and non-dust, respectively. Black vertical line shows standard
778 deviation.

779 **Figure 6.** Source apportionment of WSON from Positive Matrix Factorization for PM10 at
780 Erdemli.

781

782 **Table Captions**

783 **Table 1.** The number of negative WSON values and positive biases in coarse and fine particles
784 at Erdemli.

785 **Table 2.** The statistical summary of the WSON, NO_3^- , NH_4^+ and WSTN for aerosol (nmol N
786 m^{-3}) and rain ($\mu\text{mol N L}^{-1}$) samples collected at Erdemli from March 2014 to April 2015.

787 **Table 3.** Comparison of WSON concentrations in aerosol (nmol N m^{-3}) and rain ($\mu\text{mol N L}^{-1}$)
788 samples for different sites of the World.

789 **Table 4.** Seasonal statistical summary of the WSON, NO_3^- , NH_4^+ , WSTN (nmol N m^{-3}) and
790 nssCa^{2+} (nmol m^{-3}) in aerosol samples collected at Erdemli from March 2014 to April 2015.

791 **Table 5.** Arithmetic means along with standard deviations of WSON, NO_3^- , NH_4^+ (nmol N
792 m^{-3}) and nssCa^{2+} (nmol m^{-3}) in aerosol samples as a function of the classified airflow
793 corresponding to three day air mass back trajectories reaching at Erdemli.

794 **Table 6.** Atmospheric dry and wet deposition of WSON, NO_3^- , NH_4^+ and WSTN together
795 with their relative contributions at Erdemli during the period of March 2014 and April 2015.

796

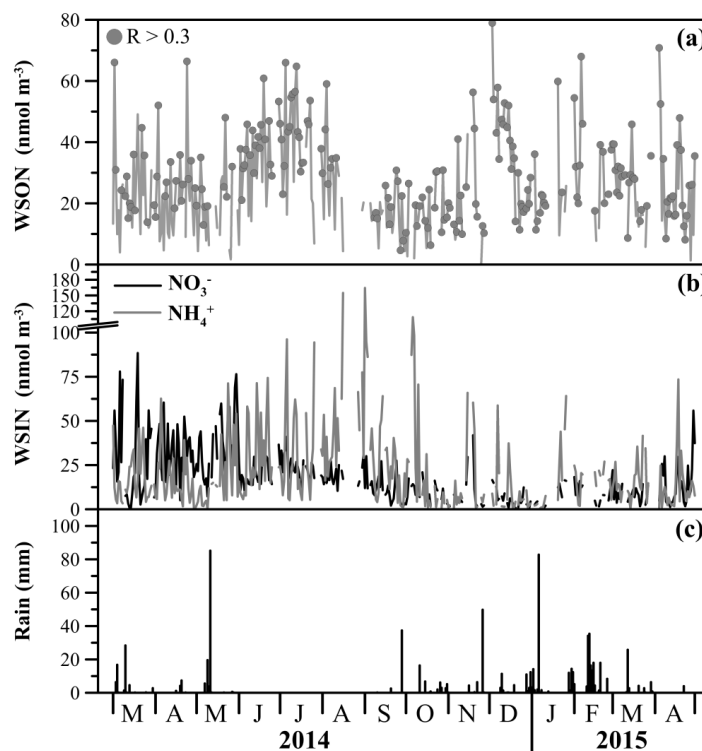
797

798

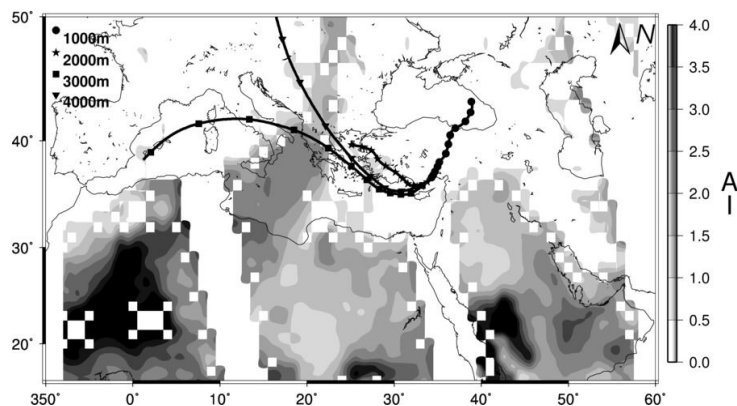


799 **Figures**

800
801



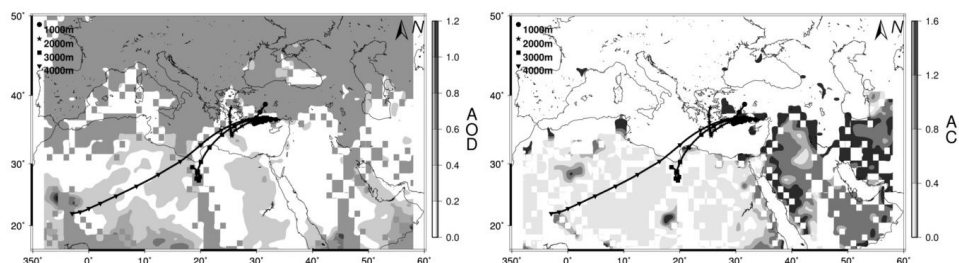
802
803 **Figure 1.** The daily variations in the concentrations of (a) WSON, (b) NO_3^- and (c) NH_4^+
804 (nmol N m^{-3}) together with rain amount (mm) from March 2014 and April 2015 for PM_{10} .
805
806



807
808 **Figure 2.** Three day back trajectories showing the transport of air masses 1000m (black circle), 2000m (black star), 3000m (black square) and 4000m (black triangle) on 5th of July
809 2014 for Erdemli. Aerosol Index (AI) from OMI (Ozone Mapping Instrument) distribution
810 also illustrated with a color bar from grey to black.
811



812

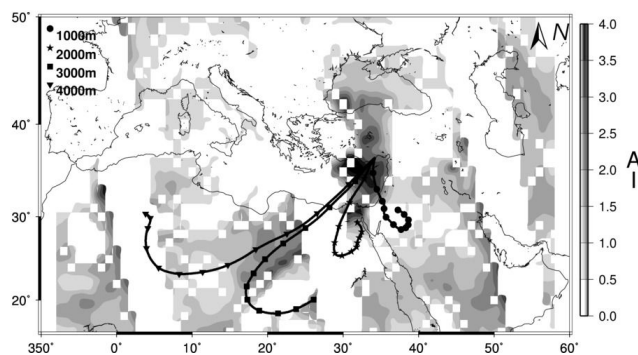


813

814 **Figure 3.** Three day back trajectories showing the transport of air masses 1000m (black circle), 2000m (black star), 3000m (black square) and 4000m (black triangle) on 20th of
815 February 2015 for Erdemli. Aerosol Optical Depth (AOD, a) and Angstrom Component (AC,
816 b) from MODIS (Moderate Resolution Imaging Spectroradiometer) distribution also
817 demonstrated with a color bar from grey to black.
818

819

820



821

822 **Figure 4.** Three day back trajectories indicating the transport of air masses 1000m (black circle), 2000m (black star), 3000m (black square) and 4000m (black triangle) on 2nd of March
823 2014 for Erdemli. Aerosol Index (AI) from OMI (Ozone Mapping Instrument) distribution
824 also illustrated with a color bar from grey to black.
825

826

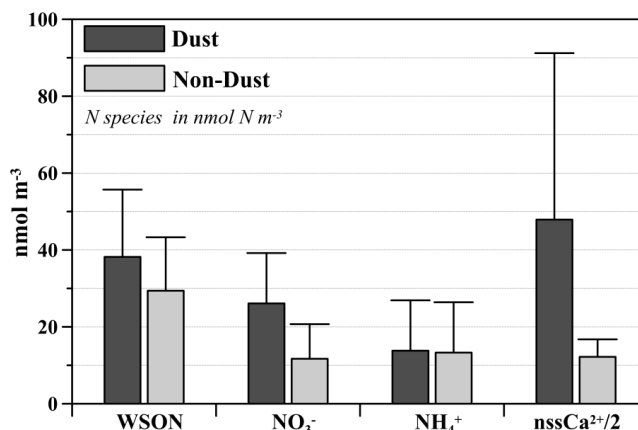
827

828

829

830

831



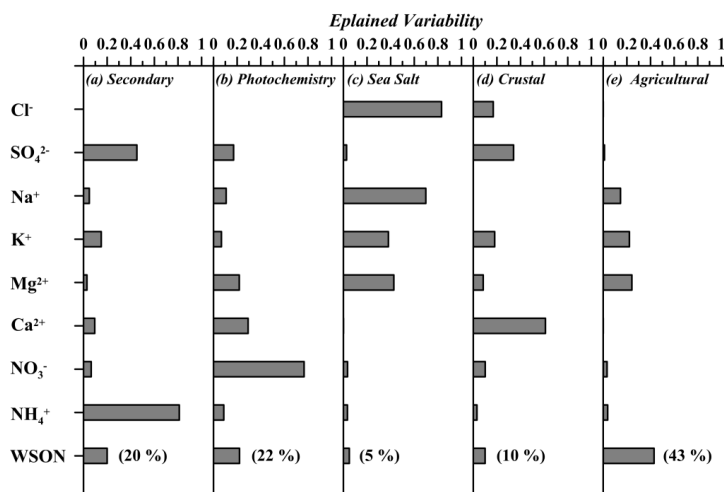
832

833 **Figure 5.** Arithmetic means together with corresponding standard deviations of WSON, NO₃⁻,
834 NH₄⁺ and nssCa²⁺ for dust and non-dust events at Erdemli site. Dark and light grey bars
835 denote arithmetic mean for dust and non-dust, respectively. Black vertical line shows standard
836 deviation.

837

838

839



840

841 **Figure 6.** Source apportionment of WSON from Positive Matrix Factorization for PM₁₀ at
842 Erdemli.

843

844

845



846

847 **Tables**

848

 849 **Table 1.** The number of negative WSON values and positive biases in coarse and fine
 850 particles at Erdemli.

	Coarse	Fine
<i>Number of Samples</i>	337	337
<i>Number of Negatives</i>	18	52
<i>SZ¹-Positive Bias (%)</i>	2	14
<i>PZ²-Positive Bias (%)</i>	8	34

 851 *1 and 2 refer to as the Substitution with Zero and the Omission of Zero, respectively.*

852

 853 **Table 2.** The statistical summary of the WSON, NO₃⁻, NH₄⁺ and WSTN for aerosol (nmol N
 854 m⁻³) and rain (μmol N L⁻¹) samples collected at Erdemli from March 2014 to April 2015.

<i>AEROSOL (nmol N m⁻³)</i>				
	<i>WSTN</i>	<i>WSON</i>	<i>NO₃⁻</i>	<i>NH₄⁺</i>
Arithmetic Mean	63.5	23.8	17.8	21.9
Standard Deviation	32.0	16.3	15.2	23.8
Minimum	9.7	-27.9	0.2	0.5
Maximum	176.5	79.0	88.4	164.4
Coarse/PM ₁₀ (%)	51	66	87	4
<i>Relative Contribution to WSTS (%)</i>		37	28	35
<i>RAIN (μmol N m⁻³)</i>				
VWM*	73.5	21.5	23.3	28.7
Minimum	24.3	-2.9	0.2	9.1
Maximum	356.2	257.2	74.6	122.6
<i>Relative Contribution to WSTS (%)</i>		29	32	39

855 *VWM refers to Volume Weighted Mean

856



857

858 **Table 3.** Comparison of WSON concentrations in aerosol (nmol N m^{-3}) and rain ($\mu\text{mol N L}^{-1}$)
859 samples for different sites of the World.

Aerosol (nmol N m^{-3})	WSON	NS	SP	Reference
Mediterranean Sea				
<i>Erdemli, Turkey</i>	23.8	674	2014-2015	This Study
<i>Erdemli, Turkey</i>	29	39	2000	Mace et al. [2003a]
<i>Finokalia, Crete</i>	17.1	65	2005-2006	Violaki and Mihalopoulos [2010]
Pacific Ocean				
<i>Hawaii</i>	4.1	16	1998	Cornell et al. [2001]
<i>Tasmania</i>	5.3	24	2000	Mace et al. [2003b]
<i>Taiwan</i>	75.9	77	2006	Chen et al. [2010]
<i>Xi'an, China ($PM_{2.5}$)</i>	300	65	2008-2009	Ho et al. [2015]
Atlantic Ocean				
<i>Barbados</i>	1.3	57	2007-2008	Zamora et al. [2011]
<i>Amazon, dry season</i>	61	37	1999	Mace et al. [2003c]
<i>Amazon, wet season</i>	3.5	27	1999	Mace et al. [2003c]
Indian Ocean				
<i>Amsterdam Island</i>	1	42	2005	Violaki et al. [2015]
Rainwater ($\mu\text{mol N L}^{-1}$)	WSON	NS	SP	Reference
Mediterranean Sea				
<i>Erdemli, Turkey</i>	21.5	23	2014-2015	This Study
<i>Erdemli, Turkey</i>	15	18	2000	Mace et al. [2003a]
<i>Finokalia, Crete</i>	18	18	2003-2006	Violaki et al. [2010]
Pacific Ocean				
<i>Tahiti*</i>	4.8	8		Cornell et al. [1998]
<i>Hawaii</i>	2.8	17	1998	Cornell et al. [2001]
<i>Tasmania</i>	7.2	6		Mace et al. [2003b]
<i>North China Plain, China</i>	103	15	2003-2005	Zhang et al. [2008]
<i>Kilauea, Hawaii</i>	6.5	20	1998	Cornell et al. [2001]
Atlantic Ocean				
<i>Bermuda</i>	5.6	5	1994	Cornell et al. [1998]
<i>Mace Head</i>	3.3	7		Cornell et al. [1998]
<i>Norwich, UK</i>	33	12		Cornell et al. [1998]
<i>Virginia, US</i>	3.1	83	1996-1999	Keene et al. [2002]
<i>Delaware, US</i>	4.2	50	1997-1999	Keene et al. [2002]
<i>New Hampshire, US</i>	0.6	12	1997	Keene et al. [2002]

860 *RC, NS and SP refer to relative contribution of WSON to WSTN, number of samples and sampling period,*
861 *respectively.*

862

863

864

865 **Table 4.** Seasonal statistical summary of the WSON, NO_3^- , NH_4^+ , WSTN (nmol N m^{-3}) and nssCa^{2+} (nmol m^{-3}) in aerosol samples collected at Erdemli from March 2014 to April 2015.

Aerosol Species	Winter	Spring	Summer	Fall
WSON	33±16	28±13	41±11	20±10
NO_3^-	7±5	15±12	21±7	9±8
NH_4^+	10±12	11±9	24±16	10±13
nssCa^{2+}	28±13	28±13	28±13	41±11
Number of Samples	47	79	46	44
Meteorology Parameter	Winter	Spring	Summer	Fall
T ($^{\circ}\text{C}$)	11±3	16±3	27±12	20±15
Rain (mm)	78	118	0.5	132
Number of Rain Events	16	16	2	15



866 **Table 5.** Arithmetic means along with standard deviations of WSON, NO_3^- , NH_4^+ (nmol N
 867 m^{-3}) and nssCa^{2+} (nmol m^{-3}) in aerosol samples as a function of the classified airflow
 868 corresponding to three day air mass back trajectories reaching at Erdemli

<i>Airflow</i>	WSON	NO_3^-	NH_4^+	nssCa^{2+}
<i>Middle East</i>	33±12	12±12	13±15	48±71
<i>North Africa</i>	36±16	18±11	12±14	46±38
<i>Turkey</i>	32±13	15±10	19±15	23±9
<i>Eastern Europe</i>	26±14	10±9	10±8	21±9
<i>Western Europe</i>	26±14	10±8	11±9	20±7
<i>Mediterranean Sea</i>	22±10	10±8	8±6	19±8

869

870

871 **Table 6.** Atmospheric dry and wet deposition of WSON, NO_3^- , NH_4^+ and WSTN together
 872 with their relative contributions at Erdemli during the period of March 2014 and April 2015.

Species	F_d ($\text{mmol N m}^{-2} \text{yr}^{-1}$)	Relative Contribution
WSON	9.8	46
NO_3^-	10.0	48
NH_4^+	1.3	6
WSTN	21.1	
Species	F_w ($\text{mmol N m}^{-2} \text{yr}^{-1}$)	Relative Contribution
WSON	10.7	29
NO_3^-	11.7	32
NH_4^+	14.3	39
WSTN	36.7	

873